

A Magnetic Suspension Theory and Its Application to the HeartQuest Ventricular Assist Device

*Chen Chen, *Brad Paden, †James Antaki, ‡Jed Ludlow, *Dave Paden,
*Randolph Crowson, and ‡Gill Bearnson

*Magnetic Moments, LLC, Goleta, California; †AntakaMatics, Inc., Pittsburgh, Pennsylvania; ‡MedQuest Products, Inc., Salt Lake City, Utah, U.S.A.

Abstract: Motivated by the design of the HeartQuest magnetically levitated left ventricular assist device, closed form expressions have been developed to compute forces and stiffnesses of magnetic suspensions. The theory applies to any combination of concentric permanent magnet rings, and its accuracy and versatility were verified by experiments. The equations adapt to spreadsheet implemen-

tation and numerical optimization, providing a powerful tool of optimal design of magnetically levitated ventricular assist devices (VADs). The method was applied to the development of the HeartQuest VAD which achieved remarkable compactness and stable operation. **Key Words:** Magnetic suspension—Design—Optimization—Blood pump—Ventricular assist device.

INTRODUCTION

The analyses of magnetic suspensions in artificial hearts are directed at two objectives. The first objective is to *understand* forces and stiffnesses in a particular suspension system. This can be accomplished with the computer-aided tools such as finite element analysis (FEA) which has been well developed since the 1950s. The second objective is to *design* a suspension to meet specific requirements for forces and stiffnesses. This represents a more difficult task and a deeper understanding of the relationships and tradeoffs between the design parameters and objectives. For example, a designer who wishes to maximize load capacity with minimal volume may find that finite-element models become overly complex and obscure important high level behavior. To meet such requirements, investigations into effective design tools are still required. Compared with FEA and other complex numerical approaches, analytical solutions are generally superior for design optimization, because they reduce numerical requirements and are suitable for spreadsheet calculations.

The existing analytical methods to compute forces and stiffnesses in magnetic bearings exhibit various complexity and levels of approximation (1–10). Backers' theory (1) represents a simple solution to stacks of alternately magnetized magnet rings that extend infinitely in the axial direction. Similar assumptions were used by Halbach, who proposed the magnetic structure known as Halbach array (2). Despite the usefulness of magnet arrays, the rotary pump is unlikely to accommodate a large number of magnets, so that the corresponding equations do not apply. Yonnet's model (3), on the other hand, deals with a single pair of magnets. However, the theory was based on the dipole model of magnet rings and thus limited to magnets with sectional dimensions smaller than the air gap length. The magnetic bearings in rotary blood pumps generally do not fall in this category either. Another set of closed-form equations used by Yonnet (4) removed such limitation on the size, but it has yet to be further developed to treat stacks of magnets with varying sizes or having a Halbach array structure. Other work in the area is typified by the development of a perturbation approach (5) to improve accuracy of bearing stiffness calculation for small-diameter magnetic rings, which has to be used together with FEA. The model proposed by Furlani (6) was based on dividing a magnet into tiny pieces and summing up forces between those pieces. The model was consid-

Received June 2002.

Presented in part at the 9th Congress of the International Society for Rotary Pumps, held August 17–20, 2001, in Seattle, Washington.

Address correspondence and reprint requests to Dr. Chen Chen, Magnetic Moments, LLC, 5735 Hollister Avenue, Suite B, Goleta, CA 93117, U.S.A. E-mail: chen@mmsb.com

ered to not fit our design needs because of the complexity.

It should be noted that the aforementioned methods and equations commonly stem from the basic principles of magnet modeling, which can be found in textbooks like Barger and Olsson (11), or Jackson (12). We started from such principles to develop a set of closed-form equations and the corresponding method to compute forces and stiffnesses of magnetic bearings specifically aimed at achieving an optimized magnetic suspension.

PRINCIPLE

We consider a magnetic suspension that is formed from concentric magnet rings of rectangular cross-section. There is no limit to the number of such magnets that form a suspension unit. Figure 1 shows two types of magnet rings under consideration, magnetized in axial or radial direction as indicated by the arrows.

Essentially, a permanent magnet can be modeled with magnetization currents which reduce to current sheets on the magnet surfaces if the interior magnetization is uniform (11,12). The bold sides of the cross-section in Fig. 1 indicate these current sheets. In this analysis, we consider a rigid magnet material (such as neodymium-iron-boron, NeFeB) that works in the range of constant magnetization, and we assume a uniform magnet material. Consequently, the model is linear, so the magnetic forces in a sophisticated suspension can be obtained by summing up forces between each pair of magnets on the two bearing races. Figure 1 lists the four basic combinations of such an elementary pair with the upper and lower rings belonging to a different race of a magnetic bearing.

On the basis of the current sheet model and the superimposition principle, the magnetic forces between two magnets can be obtained by summing up the magnetic forces between their equivalent current

sheets. Therefore, once we obtain a general force equation that accounts for a pair of current sheets, we can get a solution for any bearing configuration simply by performing a summation.

It should be noted that each elementary pair of magnet rings in Fig. 1 consists of four combinations of current sheet pairs. To derive a general equation for all these combinations, we constitute a pair of L-shaped current sheets as shown in Fig. 2. It is obvious that any of the current sheets in Fig. 1 can be derived by assigning zero length to one leg of the L. Therefore, equations for the force and stiffness between these L-shaped current sheets apply to any pair of interactive current sheets in our magnetic suspension models.

Figure 2 also indicates the geometric quantities defining the current sheet pair. A prime is used to indicate quantities relating to the bearing race that is rotating, as opposed to the stationary race. A further convention is made that the joint of the L legs for the rotating bearing race is a left bottom corner (the coordinates of which are minimal among all the points at the current sheet), and the joint point for the stationary bearing race is at the right top corner. The distances between the two current sheets may be positive, zero, or negative (Eqs. 1a and 1b).

$$\Delta r = r - r' \tag{1a}$$

$$\Delta z = z - z' \tag{1b}$$

To calculate forces between concentric magnet rings in a cylindrical coordinates system (r, z), we start with a planar two-dimensional (2-D) problem in Cartesian coordinates (x, y) which is characterized by flat infinitely long current sheets and then extend the results to the actual ring-shaped magnets. The x and y correspond to the r and z, respectively, and the same L-shaped current sheets as indicated in Fig. 2 are used as the cross-section of the planar 2-D model. Applying the classical solution to the magnetic force between 2 infinitely long current-carrying wires ([11], section 5-3) yields the following equations:

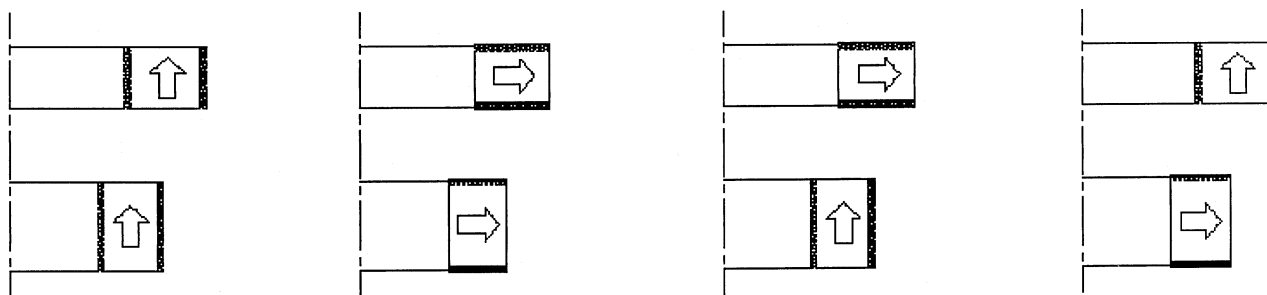


FIG. 1. Shown are basic combinations of magnet rings in a suspension unit and their equivalent current sheets (dashed line is the axis of symmetry, full section is not shown).

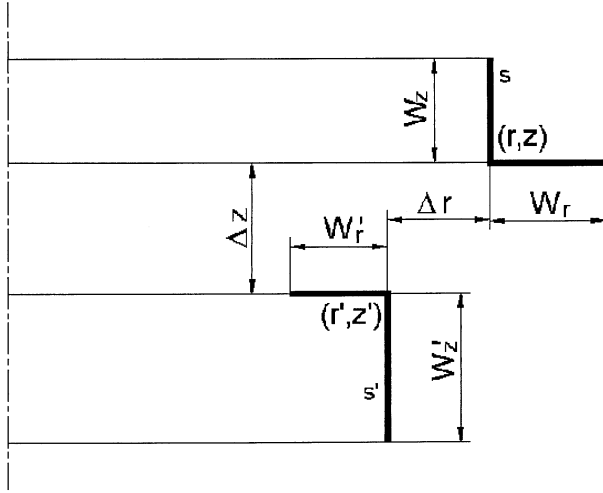


FIG. 2. A pair of L-shaped current sheets for analysis are shown.

$$f_x = \frac{\mu_0 H_C^2}{2\pi} \{U_1(W'_z, W_z, \Delta r, \Delta z) + V_1(W'_r, W_r, \Delta z, \Delta r) + U_2(W'_z, W_r, \Delta r, \Delta z) + U_2(W_z, W'_r, \Delta r, \Delta z)\} \quad (2)$$

$$f_y = \frac{\mu_0 H_C^2}{2\pi} \{V_1(W'_z, W_z, \Delta r, \Delta z) + U_1(W'_r, W_r, \Delta z, \Delta r) + U_2(W'_r, W_z, \Delta z, \Delta r) + U_2(W_r, W'_z, \Delta z, \Delta r)\} \quad (3)$$

with

$$U_1(w_1, w_2, \Delta_1, \Delta_2) = \frac{1}{2} \Delta_1 \ln\{(\Delta_1^2 + \Delta_2^2)[\Delta_1^2 + (w_1 + w_2 + \Delta_2)^2]\} - \frac{1}{2} \Delta_1 \ln\{[\Delta_1^2 + (w_2 + \Delta_2)^2][\Delta_1^2 + (w_1 + \Delta_2)^2]\} + (w_1 + \Delta_2) \tan^{-1} \frac{w_1 + \Delta_2}{\Delta_1} + (w_2 + \Delta_2) \tan^{-1} \frac{w_2 + \Delta_2}{\Delta_1} - (w_1 + w_2 + \Delta_2) \tan^{-1} \frac{w_1 + w_2 + \Delta_2}{\Delta_1} - \Delta_2 \tan^{-1} \frac{\Delta_2}{\Delta_1} \quad (4)$$

$$U_2(w_1, w_2, \Delta_1, \Delta_2) = \frac{1}{2} (w_1 + \Delta_2) \{\ln[\Delta_1^2 + (w_1 + \Delta_2)^2] - \ln[(w_2 + \Delta_1)^2 + (w_1 + \Delta_2)^2]\} + \frac{1}{2} \Delta_2 \{\ln[\Delta_2^2 + (w_2 + \Delta_1)^2] - \ln[\Delta_1^2 + \Delta_2^2]\} + (w_2 + \Delta_1) \left[\tan^{-1} \frac{\Delta_2}{w_2 + \Delta_1} - \tan^{-1} \frac{w_1 + \Delta_2}{w_2 + \Delta_1} \right] - \Delta_1 \left[\tan^{-1} \frac{\Delta_2}{\Delta_1} - \tan^{-1} \frac{w_1 + \Delta_2}{\Delta_1} \right] \quad (5)$$

$$V_1(w_1, w_2, \Delta_1, \Delta_2) = \frac{1}{2} (w_1 + \Delta_2) \ln[\Delta_1^2 + (w_1 + \Delta_2)^2] + \frac{1}{2} (w_2 + \Delta_2) \ln[\Delta_1^2 + (w_2 + \Delta_2)^2] - \frac{1}{2} (w_1 + w_2 + \Delta_2) \ln[\Delta_1^2 + (w_1 + w_2 + \Delta_2)^2] - \frac{1}{2} \Delta_2 \ln[\Delta_1^2 + \Delta_2^2] + \Delta_1 \left[\tan^{-1} \frac{w_1 + \Delta_2}{\Delta_1} + \tan^{-1} \frac{w_2 + \Delta_2}{\Delta_1} - \tan^{-1} \frac{w_1 + w_2 + \Delta_2}{\Delta_1} - \tan^{-1} \frac{\Delta_2}{\Delta_1} \right] \quad (6)$$

Here, f_x and f_y are 2 magnetic force components in the (x, y) plane, μ_0 is magnetic permeability of vacuum, and H_C is the coercive force of the magnets. Other geometric parameters are as shown in Fig. 2.

The extension of planer 2-D results to the axisymmetric situation follows the convenient way as used in other investigations (1,3,4). This results in a net zero radial force (because of concentricity). The net axial force is approximated by the planar 2-D force per unit depth multiplied by the average perimeter of the current sheet pair.

The average perimeter for the L-shaped current sheet pair is taken as the arithmetic average of the sheet legs:

$$R_{aver} = \frac{1}{2} (r + r') + \frac{1}{4} (W_r - W'_r) \quad (7)$$

Therefore, the net axial force on the current sheet is

$$F_z = \mu_0 H_C^2 R_{aver} \{V_1(W'_z, W_z, \Delta r, \Delta z) + U_1(W'_r, W_r, \Delta z, \Delta r) + U_2(W'_r, W_z, \Delta r, \Delta z) + U_2(W_r, W'_z, \Delta z, \Delta r)\} \quad (8)$$

Consider the stiffness of the suspension. The axial stiffness in the L-shaped current sheet pair is obtained by partial differentiation of F_z with respect to Δz :

$$k_z = - \frac{\partial F_z}{\partial \Delta z} = \mu_0 H_C^2 R_{aver} \{S_1(W'_z, W_z, \Delta r, \Delta z) - S_1(W'_r, W_r, \Delta z, \Delta r) - S_2(W_r, W'_z, \Delta z, \Delta r) - S_2(W'_r, W_z, \Delta z, \Delta r)\} \quad (9)$$

with

$$S_1(w_1, w_2, \Delta_1, \Delta_2) = \frac{1}{2} \ln\{(\Delta_1^2 + \Delta_2^2)[\Delta_1^2 + (w_1 + w_2 + \Delta_2)^2]\} - \frac{1}{2} \ln\{[\Delta_1^2 + (w_2 + \Delta_2)^2][\Delta_1^2 + (w_1 + \Delta_2)^2]\} \quad (10)$$

$$S_2(w_1, w_2, \Delta_1, \Delta_2) = \tan^{-1} \frac{\Delta_2}{w_2 + \Delta_1} + \tan^{-1} \frac{w_1 + \Delta_2}{\Delta_1} - \tan^{-1} \frac{w_1 + \Delta_2}{w_2 + \Delta_1} - \tan^{-1} \frac{\Delta_2}{\Delta_1} \quad (11)$$

The radial stiffness is obtained through application of the Earnshaw's theorem (3,4) which implies that the radial stiffness is half of the axial stiffness in an axisymmetric construction. That is

$$k_r = -\frac{k_z}{2} \quad (12)$$

Finally, the angular stiffness with respect to axis r (normal to the z axial and passing through the origin) is obtained as

$$k_\varphi = \left[-R_{aver}^2 + \left(z + \frac{W_z}{2} \right)^2 \right] k_r \quad (13)$$

where z is the coordinate of the current sheet corner (Fig. 2). It should be noted that the coordinate system is placed in such a way that the origin coincides with the so-called bearing center of the suspension. The bearing center can be found by computing moments of every current sheet comprising the whole suspension.

In summary, the forces and stiffnesses in a magnetic suspension are calculated according to the following procedure. First, replace the magnet rings with equivalent current sheets. Second, compute magnetic force and stiffnesses between each pair of current sheets with the preceding equations. For a suspension composed of n current sheets in each race, there are $n \times n$ such interaction forces to be calculated. Finally, sum up all those interactive forces and stiffnesses to get the net force and stiffnesses of the suspension unit.

VERIFICATION

The preceding equations and method were applied to a great number of design trials. For several of them, FEA and/or experiments were performed to verify the theory. A typical FEA study was performed on a Halbach array structure that was optimized with the aid of the theory. The study showed less than 3% errors for all the force and stiffness

components between the FEA and the analytical results.

Experimental verification was carried out with a specially designed test fixture which consists of a positioning stage and a force cell. The stage carries rotor components, and the force cell holds the stator components. By moving the stage, relative displacements between the rotor and stator components are produced. Accuracy of linear position is kept within $2.54 \mu\text{m}$ and that of angular positioning is 0.0001 rad . The force cell is a six degree-of-freedom force and torque sensor with accuracy of 0.025 Nt for forces and 0.5 Nt-mm for torque measurements.

Several different magnetic suspension configurations were tested for forces and stiffnesses using the test fixture. These corresponded to candidate designs for the HeartQuest blood pump. Most of the tests presented forces and stiffnesses within 15% error from the analytical values which overestimated the actual values. This was attributed to the imperfections in magnet material and mechanical tolerances that were not taken into account in the theory. The FEA and experimental studies verified applicability of the analytical solution to the design of magnetic suspension system in rotary blood pumps.

APPLICATION TO HEARTQUEST BLOOD PUMP DESIGN

The HeartQuest VAD is a magnetically levitated centrifugal pump designed for left ventricular assistance. The design philosophy of the HeartQuest VAD is to achieve system optimization by means of the application of mathematical modeling and optimization. The pump is divided into subsystems, including passive (permanent magnet) suspension, active suspension (voice coil actuator), electric motor, mainline flow, and clearance flow. Closed-form design equations were developed for each of the subsystems. In addition, rigid-body rotordynamic analysis was performed to ensure stability of the suspension.

Because the preceding magnetic bearing design theory is capable of dealing with an arbitrary number of magnet rings with different size and magnetization, it enabled investigation of a variety of system topologies. The equations were embedded into spreadsheets which perform calculations automatically and allow for constrained optimization using generalized reduced gradient (GRG2) nonlinear optimization embedded in the Microsoft Excel. In accordance with the current sheet model, a matrix structure was used for the force or stiffness calculation. Each cell in the matrix calculates one interactive force or stiffness between one pair of current

sheets, and a sum of all the cells gives the net force or stiffness of the suspension unit.

The dimensions of each magnet ring were designated as design variables subject to optimization. The objectives were to maximize radial stiffness and moment stiffness under certain constraints of the space available to accommodate the magnets. These constraints came from the requirement of the whole system, as well as the relationship of the suspension to the other subsystems. The numerical optimization algorithm was demonstrated to work properly for all suspension topologies investigated.

The optimal design process has yielded a prototype HeartQuest blood pump. Its impeller consists of blades sitting on an annular hub. The housing consists of a central spindle, a bottom, and an outer peripheral structure that surround the impeller hub. Magnet rings inside the spindle cooperate with magnet rings in the impeller hub to provide radial suspension, and magnet rings in the housing outer peripheral construction work with the corresponding magnets in the impeller hub to provide titling suspension. Complex magnetic stacks were used to increase the suspension stiffnesses. The hub also contains rotor components of the electric motor. The design optimization resulted in a hub 8 mm thick with 50 mm outer diameter, with all suspension and motor components in the rotor accommodated. The suspension achieved more than a 40% margin relative to the first critical speed for both transverse and precession rotor resonance. It also possessed sufficient stiffnesses to reject external disturbances, including fluid loads and shock.

Force and stiffness tests were performed on the prototype with the aforementioned test fixture. The tests demonstrated that the actual radial and axial stiffnesses were 15% less than the optimal design values whereas the moment stiffness was 5% more than the design value. These are acceptable levels of error considering the safety margin built into the design. Therefore, the application of the present theory to the HeartQuest blood pump design has demonstrated remarkable accuracy and versatility. The theory's characteristics of adapting to optimization mathematics enabled design optimization.

Several assumptions with respect to the material and geometry, as stated in section 2, lead to practical limitations for the present method. In particular, it does not apply to systems involving ferromagnetic material which has significant influence on the passive suspension. The magnetization in a ferromagnetic material varies with applied magnetic field, and this requires more complicated models, rather than the current sheet model, for the ferromagnetic construction. Although ferromagnetic material can be treated as a mirror for permanent magnet images in some instances, this article is not intended for further discussion on such treatment. As far as the HeartQuest blood pump is concerned, the design process has justified a topology of virtually iron-free magnetic suspension, and ferromagnetic materials in the other part of the pump have had a minor influence on the suspension, as demonstrated by FEA and experiments.

REFERENCES

1. Backers FT. A magnetic journal bearing. *Philips Tech Rev* 1960/61;22:232-8.
2. Halbach K. Application of permanent magnets in accelerators and electron storage rings. *J Appl Phys* 1985;57:3605-8.
3. Yonnet JP. Permanent magnet bearings and couplings. *IEEE Trans Magn* 1981;17:1169-73.
4. Yonnet JP. Analytical calculation of magnetic bearings. *Proceedings of the 5th International Workshop on Rare Earth-Cobalt Permanent Magnets and Their Applications* 1981; 199-216.
5. Marinescu M, Marinescu N. A new improved method for computation of radial stiffness of permanent magnet bearings. *IEEE Trans Magn* 1994;30:3491-4.
6. Furlani EP. A formula for the levitation force between magnetic disks. *IEEE Trans Magn* 1993;29:4165-9.
7. Akoun G, Yonnet JP. 3D analytical calculation of the forces and exerted between two cuboidal magnets. *IEEE Trans Magn* 1984;20:1962-4.
8. Delamare J, Yonnet JP, Rulliere E. A compact magnetic suspension with only one axis control. *IEEE Trans Magn* 1994; 30:4746-8.
9. Antila MJ. The load capacity and stiffness of the axial permanent magnet bearings. *Proceedings of the 4th International Symposium on Magnetic Bearings* 1994;287-291.
10. Krist P, Gerber R, Boehm J, et al. Ponderomotive interactions between arrays of permanently magnetized rectangular prisma. *IEEE Trans Magn* 1993;29:2935-7.
11. Barger VD, Olsson MG. *Classical Electricity and Magnetism: A Contemporary Perspective*. New York: Allyn and Bacon, Inc., 1987.
12. Jackson JD. *Classical Electrodynamics*, 2nd ed., New York: John Wiley & Sons, 1975.